Methylphenidate Effects on Brain Activity as a Function of *SLC6A3* Genotype and Striatal Dopamine Transporter Availability

Anna-Maria Kasparbauer[1], Dan Rujescu[2], Michael Riedel[3,4], Oliver Pogarell[3], Anna Costa[3], Thomas Meindl[5], Christian la Fougère[6,7] and Ulrich Ettinger*[,1]

[1]*Department of Psychology, University of Bonn, Bonn, Germany;* [2]*Department of Psychiatry, University of Halle, Halle, Germany;* [3]*Department of Psychiatry, University of Munich, Munich, Germany;* [4]*Clinic for Psychiatry, Psychotherapy, Gerontopsychiatry and Neurology, Rottweil, Germany;* [5]*Institute of Clinical Radiology, University of Munich, Munich, Germany;* [6]*Department of Nuclear Medicine, University of Munich, Munich, Germany;* [7]*Department of Nuclear Medicine, University of Tübingen, Tübingen, Germany*

We pharmacologically challenged catecholamine reuptake, using methylphenidate, to investigate its effects on brain activity during a motor response inhibition task as a function of the 3′-UTR variable number of tandem repeats (VNTR) polymorphism of the dopamine transporter (DAT) gene (*SLC6A3*) and the availability of DATs in the striatum. We measured the cerebral hemodynamic response of 50 healthy males during a Go/No-Go task, a measure of cognitive control, under the influence of 40 mg methylphenidate and placebo using 3T functional magnetic resonance imaging. Subjects were grouped into 9-repeat (9R) carriers and 10/10 homozygotes on the basis of the *SLC6A3* VNTR. During successful no-go trials compared with oddball trials, methylphenidate induced an increase of blood oxygen level-dependent (BOLD) signal for carriers of the *SLC6A3* 9R allele but a decrease in 10/10 homozygotes in a thalamocortical network. The same pattern was observed in caudate and inferior frontal gyrus when successful no-go trials were compared with successful go trials. We additionally investigated in a subset of 35 participants whether baseline striatal DAT availability, ascertained with ^{123}I-FP-CIT single photon emission computed tomography, predicted the amount of methylphenidate-induced change in hemodynamic response or behavior. Striatal DAT availability was nominally greater in 9R carriers compared with 10/10 homozygotes ($d = 0.40$), in line with meta-analyses, but did not predict BOLD or behavioral changes following MPH administration. We conclude that the effects of acute MPH administration on brain activation are dependent on DAT genotype, with 9R carriers showing enhanced BOLD following administration of a prodopaminergic compound.

Neuropsychopharmacology (2015) **40**, 736–745; doi:10.1038/npp.2014.240; published online 8 October 2014

INTRODUCTION

Dopamine (DA) has a key role in cognitive control, viz the ability to bias information processing according to goal relevance. Specifically, DA is thought to influence striatal and prefrontal activity during cognitive control (Bari and Robbins, 2013).

One important function of cognitive control is inhibition, viz the suppression of inappropriate thoughts and actions. The ability to suppress prepotent motor responses is commonly studied using the Go/No-Go paradigm. This task requires a motor response to a frequent go stimulus, but response suppression to an infrequent no-go stimulus (Dalley *et al*, 2011). Blood oxygen level-dependent (BOLD) functional magnetic resonance imaging (fMRI) studies have identified the striatum and prefrontal cortex (PFC) to underlie performance (Bari and Robbins, 2013).

Poor Go/No-Go performance is observed in patients with ADHD (Bezdjian *et al*, 2009), schizophrenia (Weisbrod *et al*, 2000), and Parkinson's disease (Cooper *et al*, 1994). Methylphenidate (MPH), a catecholamine reuptake inhibitor, improves impaired inhibition in patients (Coghill *et al*, 2014) and enhances cognitive performance in healthy subjects (Linssen *et al*, 2014). MPH indirectly elevates extracellular concentrations of DA levels in striatal (Volkow *et al*, 1994) and extrastriatal (Montgomery *et al*, 2007) regions by blockage of DA transporters (DAT), while additionally blocking noradrenaline transporters.

Although DA increases tend to improve cognition, individual differences in response to dopaminergic compounds are also observed (Mehta, 2002). Clarifying the predictors of this variance is important not only to improve our mechanistic understanding of these compounds but also to identify markers of treatment response in clinical populations such as ADHD (Kambeitz *et al*, 2014).

Previous research has identified the individual's molecular baseline DA level as a potent predictor of dopaminergic drug effects (Cools and D'Esposito, 2011; Goldman-Rakic *et al*, 2000). Crucial evidence for such baseline dependency comes from pharmacogenetic studies of DA gene polymorphisms as predictors of drug effects (Cohen *et al*, 2007; Mattay *et al*, 2003). For example, after amphetamine administration, reduced brain activity and improved performance was shown for individuals thought to have low baseline DA levels in PFC according to their $val^{158}met$ polymorphism of the *catechol-O-methyltransferase* (*COMT*) gene. The same compound impaired performance and increased brain activity in individuals with the allele associated with high baseline DA levels (Mattay *et al*, 2003).

However, COMT is scarce in the striatum, where DATs predominantly terminate dopaminergic signaling (Gainetdinov and Caron, 2003). The gene coding for the DAT (*SLC6A3*; OMIM 126455) is located on chromosome 5p15.3 and includes a variable number of tandem repeats (VNTR) polymorphism of a 40 base-pair sequence in the 3'-untranslated region (3'-UTR). The most common polymorphisms are the 9/10 and 10/10 forms (Vandenbergh *et al*, 1992).

The VNTR has been investigated in relation to MPH treatment in ADHD patients. A recent meta-analysis failed to confirm the VNTR polymorphism as significant overall predictor of treatment success (Kambeitz *et al*, 2014), but suggested that 10-repeat (10R) homozygotes may show less improvement than other genotypes in naturalistic trials.

However, only few pharmacogenetic studies are available on the *SLC6A3* genotype-dependent cognitive or neural response to MPH. Loo *et al* (2003) found the VNTR to predict MPH effects on behavioral performance and the electroencephalographic response in children with ADHD. Further evidence of the influence of the VNTR on MPH effects comes from a transcranial magnetic stimulation study of cortical inhibitory activity in ADHD (Gilbert *et al*, 2006). However, there are no investigations of *SLC6A3* in MPH-induced changes in BOLD at all and none on its role in MPH-induced changes in cognition in healthy participants.

In addition to genetic predictors, DAT binding characteristics may provide another potential baseline predictor of MPH response. Single photon emission computed tomography (SPECT) quantified striatal DAT availability has previously been associated with treatment outcome in ADHD (la Fougère *et al*, 2006). However, no studies have investigated DAT availability as predictor of MPH effects on neural or cognitive measures. Recent meta-analyses attribute higher striatal DAT availability to *SLC6A3* 9R carriers (Costa *et al*, 2011; Faraone *et al*, 2014), calling for a combination of these two potential predictors.

We have previously shown MPH effects on striatal BOLD during a Go/No-Go task (Costa *et al*, 2013b). Here, we extend these findings by combining genetic and molecular information to explore the MPH-induced changes in dependency of DAT genotype and availability. We grouped participants according to *SLC6A3* VTNR polymorphism (9R carriers or 10/10 homozygotes) and measured the amount of striatal DAT for a subset of participants using ^{123}I-FP-CIT SPECT. Taken together, these genetic and molecular markers allowed a thorough investigation of interindividual differences in DA baseline levels as predictor of MPH response.

We expected that MPH would lead to alterations in frontostriatal networks (Costa *et al*, 2013b; Rubia *et al*, 2011). Concerning *SLC6A3* genotype, in line with previous meta-analyses, we expected higher striatal DAT binding for 9R carriers in comparison with 10/10 homozygotes (Costa *et al*, 2011; Faraone *et al*, 2014). Furthermore, we speculated that higher DAT availability would be predictive of behavioral improvement following MPH administration, as previously shown in molecular imaging (la Fougère *et al*, 2006) and genetic (Kambeitz *et al*, 2014) studies.

MATERIALS AND METHODS

Participants

Healthy, right-handed, nonsmoking, men were recruited through local advertisements. Only Caucasian participants were included to minimize genetic heterogeneity. Participants provided written informed consent. The study was approved by the ethics committee of the Faculty of Medicine of the University of Munich.

Screening Procedure

Participants first underwent a screening including EEG, ECG, blood test, and medical interview to exclude any previous or current psychiatric or neurologic illness including alcohol and drug abuse. Further exclusion criteria were any current medication, current medical illness, first-degree relative with schizophrenia or ADHD, metallic implants, and claustrophobia.

Experimental Procedure

A randomized, double-blind, placebo-controlled, within-subjects design was used (Costa *et al*, 2013b). Each participant was scanned two times over ∼1 week at the same time of day. Participants abstained from alcohol 24 h before scanning.

During each session, two capsules containing either an overall dose of 40 mg MPH or placebo (lactose; PLC) were administered orally, comparable to previous studies of healthy participants (Linssen *et al*, 2014). Following capsule administration, participants were not allowed to eat or drink, with the exception of water. fMRI started 60 min after capsule administration.

Go/No-Go Task and Analysis

The event-related Go/No-Go task (Chikazoe *et al*, 2009a) involved 200 go trials, 30 oddball trials, and 30 no-go trials. Each trial consisted of a colored circle presented for 500 ms on black background in the middle of the screen, followed by 1300 ms (jittered 1100–1500 ms) of black background. Go trials were indicated by a gray circle. No-go and oddball trials were indicated by yellow or blue circles, counterbalanced across participants. Trial order was quasirandomized with 3, 4, or 5 go trials between no-go and oddball trials and between no-go trials. Participants had to press a button with their right index finger on go and oddball trials, but had to withhold the response on no-go trials.

Dependent variables were percentage of no-go commission errors, reaction times (RTs) of errors as well as correct go and oddball responses, and the intraindividual coefficient of variation (ICV) of RTs during incorrect no-go, correct go, and correct oddball trials. ICV was calculated as follows: ICV = standard deviation (SD) RT/mean RT (Nandam et al, 2011). RTs smaller than 200 ms and higher than the individual mean RT plus 2.5 individual SD were excluded.

A 2×2 mixed-model analysis of variance (ANOVA) was carried out for commission errors in SPSS Statistics 21 (IBM SPSS) using Drug (MPH, PLC) as within-subject factor and Genotype (9R, 10/10) as between-subject factor. ICVs were analyzed by a $2 \times 2 \times 2$ mixed-model ANOVA with Drug and Trial Type (go, odd, incorrect no-go) as within-subject factors and the between-subject factor Genotype.

Greenhouse Geisser correction was applied if assumption of sphericity was violated.

fMRI Data Acquisition and Analysis

T2*-weighted whole-brain MR echo planar images of the BOLD response were collected on a Siemens Verio scanner at 3 T field strength. Two hundred and sixty-four functional images were acquired with a repetition time of 1.8 s. The first four volumes were discarded to allow for establishment of steady-state longitudinal magnetization. Each image volume compromised 28 axial slices, each 4 mm thick with an interslice gap of 0.8 mm and an in-plane resolution of 3×3 mm^2. Flip angle was 80° and echo time was 30 ms. Slices were acquired inferior to superior parallel to the AC–PC line.

Data were processed using SPM8 (http://www.fil.ion.ucl.ac.uk/spm/) running in MATLAB R2010a (The MathWorks). Images were aligned to the first image in the time series, normalized to the MNI template, and spatially smoothed using an 8 mm full-width-at-half-maximum Gaussian filter. Data were high-pass filtered (128 s) and stimulus onsets were modeled as events at individual subject level. The conditions (1) correct no-go trials, (2) incorrect no-go trials, (3) correct oddball trials, (4) incorrect oddball trials, and (5) incorrect go trials were modeled using a synthetic canonical hemodynamic response function. Go trials served as baseline (Chamberlain et al, 2009; Chikazoe et al, 2009a). Individual realignment parameters were included as multiple regressors.

We focused on the first-level contrast correct no-go vs correct odd as indicator of successful inhibition without the confounding influences of attentional capture (Chikazoe et al, 2009b; Criaud and Boulinguez, 2013). For comparability purposes, we also calculated the following first-level contrasts: (i) correct no-go > baseline, (ii) incorrect no-go > baseline, (iii) correct odd > baseline, and (iv) correct no-go > incorrect no-go.

For all analyses, the threshold for statistical significance was set at $P < 0.05$ and family-wise error (FWE) corrected at the cluster level and at $P < 0.001$ uncorrected at voxel level across the whole brain. At group level, we used the framework of the general linear model applying a flexible factorial model with the within-subject factor Drug (MPH, PLC) and the between-subject factor Genotype (9R, 10/10).

DNA Extraction and Genotyping

DNA was extracted from 3 ml saliva using QIAamp DNA Blood Midi Kit (Qiagen, Germany). The following primers were used: forward, 5′-TGTGGTGTAGGGAACGGCCTGAG-3′; reverse, 5′-CTTCCTGGAGGTCACGGCTCAAGG-3′ (Vandenbergh et al, 1992). A PCR reaction containing 50 ng DNA, 10 pmol of each primer, 5 U Taq polymerase (Fermentas, Vilnius, Lithuania), and 100 mM dNTP Mix (Fermentas) was carried out with buffer supplied by the manufacturer in a final volume of 20 µl. Amplification was carried out in a Thermocycler (Eppendorf, Hamburg, Germany) using the following conditions: initial denaturation at 95 °C for 5 min, 35 cycles of denaturation at 95 °C for 30 s, annealing at 61 °C for 30 s, and elongation at 72 °C for 90 sec following a final elongation at 72 °C for 3 min. PCR products were separated on 2% agarose gel by electrophoresis and visualized by ethidium bromide staining and UV fluorescence.

SPECT Data Acquisition and Analysis

A SPECT scan was performed on a separate occasion, with an MPH washout period of at least 1 week. These data served to measure baseline DAT-specific binding independent of MPH challenge.

SPECT scans were acquired 4 h after intravenous injection of ~185 MBq ^{123}I-FP-CIT (DaTSCAN; GE Healthcare, Amersham, UK) using a Prism 3000 triple-headed gamma camera (Philips, formerly by Picker, Cleveland, OH, USA) equipped with high-resolution fan beam collimators (120 projections at 60 s/view; total scan time 43 min) (Costa et al, 2013a).

Projection data were checked for motion. Images were reconstructed by filtered back-projection (Butterworth 3-dimensional (3-D) postfilter; 0.60 cycles/cm, 5th order) and corrected for attenuation (Chang, 1978).

Data were semiquantitatively evaluated using a modified version of the Brain Analysis Software (BRASS, version 3.5; Hermes Medical Solutions) and standardized 3-D volumes of interest (VOIs). This software has been validated previously for SPECT with ^{123}I-IBZM (Radau et al, 2000) and ^{123}I-FP-CIT (Koch et al, 2005). It automatically performs a multistep registration of individual images to an ^{18}F-DMFP template for healthy controls. The individual images are initially fitted to the template by means of a principal-axes technique, the iterative simplex algorithm with nine degree of freedom.

VOIs were finely adjusted to the individual image by further automatic registrations, using six degree of freedom. For each participant, three VOIs were obtained: whole striatum, caudate, and putamen. The analysis of the different compartment of the striatum, for example, the differentiation of putamen and caudate is performed routinely in the Department of Nuclear Medicine for all DaTSCAN examinations and did not cause an additional effort in our analysis. The rationale for the subsegmentation of the striatum into putamen and caudate stems from previous observations of selective effects of disease (la Fougère et al, 2010) and MPH (Costa et al, 2013b) on putamen but not caudate.

An additional VOI was defined in the occipital cortex of the template image. Accurate VOI placement was verified

and manually adjusted when necessary. This procedure has been described in more detail elsewhere for ^{123}I-FP-CIT (Koch et al, 2007) SPECT and ^{18}F-DMFP (la Fougère et al, 2010) PET. Specific binding in the striatum corrected for unspecific uptake in the occipital cortex was calculated according to the following formula: (striatum − occipital cortex)/occipital cortex. Binding data for putamen and caudate were obtained accordingly.

For statistical analysis, we first performed a repeated-measures ANOVA with Region (caudate, putamen) as within-subject factor and Genotype as between-subject factor using SPSS. Second, SPECT data from the striatum, caudate, and putamen (ie, three VOIs) were entered in separate analyses as covariate into the flexible factorial model in SPM8, as described above. Third, we analyzed the fMRI data of the SPECT sample without the factor Genotype but with SPECT data as covariate, separately for data from the striatum, caudate and putamen, to obtain neural correlates in which DAT availability modulates brain activity during any of the task conditions independent of genotype effects.

RESULTS

Participants

The sample comprised 50 healthy, right-handed, male, Caucasian nonsmokers (age mean ± SD: 23.72 ± 3.05 years; range: 18–31 years), identical to the subsample that was used for the Go/No-Go task analysis in Costa et al (2013b). Twenty-eight participants were 10/10 homozygotes. There were also carriers of the 9/10 genotype ($N_{9/10} = 15$), 9/9 homozygotes ($N_{9/9} = 5$), and 9/11 heterozygotes ($N_{9/11} = 2$). These latter groups were combined into the 9R carriers group (Costa et al, 2011; Kambeitz et al, 2014).

Thirty-five participants returned for SPECT ($N_{9/10} = 13$; $N_{9/9} = 4$; $N_{9/11} = 2$; $N_{10/10} = 16$).

Behavioral Results

The percentage of excluded trials is summarized in Supplementary Materials. Descriptive statistics are given in Table 1.

There was a main effect of Trial Type on ICVs with higher variability in incorrect no-go trials than in other conditions ($F(1.043, 50.076) = 13.43$; $P = 0.001$). The same effect was observed in the SPECT subsample ($F(1.029, 33.962) = 8.11$; $P = 0.007$). There were no other main or interaction effects on any behavioral variables (all $P > 0.094$).

Neuroimaging Results

fMRI main effects of task and drug. Effects of Task and Drug and their interactions are discussed in Costa et al (2013b) and illustrated in Supplementary Materials (Supplementary Figures S1–S5). Briefly, the only significant effect of Drug was an increase in BOLD with MPH in the right putamen during incorrect no-go, but not during correct no-go trials (Supplementary Figure S5).

Association of genotype with fMRI response to MPH. The flexible factorial model on the contrast correct no-go > correct odd yielded a significant Drug-by-Genotype interaction for cortical clusters associated with the global No-Go network (Criaud and Boulinguez, 2013): right supramarginal gyrus, right middle frontal gyrus, right precentral gyrus, bilateral cingulate gyrus, and right middle temporal gyrus. The interaction was also observed in bilateral thalamic regions, cerebellum, and occipital cortices (Figure 1). Table 2 lists significant clusters with described statistical significance threshold.

We also observed a qualitatively similar interaction between Drug and Genotype for the contrast correct no-go > baseline in left inferior frontal gyrus and right thalamus (see Supplementary Figure S6).

The statistical parametric maps presenting Drug-by-Genotype interaction clusters for the two successful inhibition contrasts (correct no-go > correct odd and correct no-go > baseline) overlapped in the right thalamus (Supplementary Figure S7).

In the SPECT subsample, we observed the same interactions for the contrasts correct no-go > correct odd and correct no-go > baseline; however, because of the smaller sample size, they achieved significance using a voxel-wise threshold of $P < 0.005$ uncorrected and the FWE-corrected cluster-wise threshold of $P < 0.05$ (Supplementary Figure S8).

To further investigate the nature of the observed interaction effect, mean parameter estimates were extracted for each cluster using MarsBaR (http://sourceforge.net/projects/marsbar). In each cluster, the Drug-by-Genotype interaction arose through an increase of BOLD from PLC to MPH for 9R carriers and a decrease for 10/10 homozygotes (Figure 2). Also, it becomes apparent from Figure 2 that BOLD in the PLC condition was higher for 10/10 homozygotes compared with 9R carriers, whereas the opposite pattern was observed in the MPH condition.

Association of SPECT and fMRI. There was a main effect of Region ($F(1,33) = 179.76$; $P < 0.001$) with greater binding of DAT in the caudate compared with putamen. Although there was no main effect of Genotype ($F(1,33) = 1.08$; $P = 0.31$), 9R carriers had numerically higher ratios with a medium effect size (striatum: $d = 0.40$; caudate: $d = 0.34$; putamen: $d = 0.32$; Table 1). The interaction between Region and Genotype was not significant ($P = 0.59$). Adding SPECT ratios as covariates in separate flexible factorial models did not alter the results for any of the contrasts, even when excluding Genotype. We additionally correlated SPECT binding with mean BOLD signal from clusters extracted with MarsBaR for the whole sample and separately by Genotype. There were no significant correlations between BOLD and SPECT values.

DISCUSSION

MPH is a widely prescribed compound with effects on inhibitory control in ADHD patients as well as healthy controls. Here, we aimed to identify genetic and molecular predictors of MPH-induced changes in brain activity during response inhibition. Our sample was divided according to their 40 base-pair VNTR polymorphism in the 3′-UTR of the *SLC6A3* gene. Striatal DAT availability was measured via ^{123}I-FP-CIT SPECT.

Table 1 Age, Striatal SPECT Ratio, and Behavioral Variables According to Genotype Group and Drug

Genotype	All (N = 50)				SPECT subsample (N = 35)			
	10/10 (N = 28)		9R (N = 22)		10/10 (N = 16)		9R (N = 19)	
	Mean	SD	Mean	SD	Mean	SD	Mean	SD
Age (years)	24.29	(3.32)	23.00	(2.56)	24.81	(3.89)	23.00	(2.75)
Specific striatal binding	—	—	—	—	2.97	(0.19)	3.08	(0.33)
Caudate-specific binding					3.12	(0.24)	3.23	(0.38)
Putamen-specific binding					2.81	(0.14)	2.89	(0.31)
Go/No-Go variables								
Methylphenidate								
Percentage of incorrect no-go	16.50	(11.12)	16.97	(9.05)	13.69	(7.74)	16.84	(9.30)
Percentage of incorrect go	0.68	(0.82)	0.68	(1.21)	0.50	(0.73)	0.74	(1.20)
Percentage of incorrect odd	0.25	(1.32)	1.14	(2.35)	0	(0)	1.32	(2.50)
Mean RT correct go	316.36	(30.52)	321.51	(44.18)	319.30	(35.14)	319.64	(42.41)
Mean RT incorrect no-go	395.67	(140.66)	417.84	(238.02)	426.06	(163.67)	384.28	(202.68)
Mean RT correct odd	380.40	(49.45)	376.03	(53.21)	382.17	(42.72)	372.08	(48.51)
SD RT correct go	48.07	(12.63)	49.71	(15.17)	50.42	(13.81)	49.74	(15.33)
SD RT incorrect no-go[a]	158.88	(228.45)	183.54	(338.41)	221.01	(293.26)	144.83	(279.49)
SD RT correct odd	81.49	(25.13)	82.62	(28.92)	78.11	(16.94)	80.03	(24.40)
ICV correct go	0.15	(0.03)	0.15	(0.03)	0.16	(0.03)	0.15	(0.01)
ICV incorrect no-go[a]	0.32	(0.33)	0.27	(0.32)	0.40	(0.41)	0.24	(0.28)
ICV correct odd	0.21	(0.057)	0.22	(0.03)	0.21	(0.05)	0.21	(0.06)
Placebo								
Percentage incorrect no-go	17.46	(8.92)	20.45	(12.00)	14.50	(8.17)	20.42	(12.84)
Percentage of incorrect go	0.50	(0.06)	1.00	(1.50)	0.56	(0.63)	1.05	(1.58)
Percentage of incorrect odd	0.46	(1.50)	0.55	(1.12)	0.38	(1.03)	0.63	(1.26)
Mean RT correct go	319.10	(33.13)	320.07	(35.19)	330.20	(37.81)	319.96	(34.68)
Mean RT incorrect no-go	446.71	(322.47)	362.94	(92.60)	479.95	(396.45)	360.40	(96.04)
Mean RT correct odd	369.35	(57.99)	370.80	(48.62)	388.16	(65.43)	366.58	(45.29)
SD RT correct go	54.01	(15.15)	49.14	(14.25)	58.12	(18.25)	49.51	(15.13)
SD RT incorrect no-go[a]	194.83	(268.96)	136.62	(184.15)	174.09	(241.08)	139.72	(198.52)
SD RT correct odd	73.51	(26.64)	75.46	(17.33)	77.88	(24.95)	74.64	(17.89)
ICV correct go	0.17	(0.03)	0.15	(0.03)	0.17	(0.04)	0.15	(0.03)
ICV incorrect no-go[a]	0.37	(0.37)	0.32	(0.34)	0.36	(0.38)	0.32	(0.36)
ICV correct odd	0.19	(0.05)	0.20	(0.03)	0.20	(0.04)	0.20	(0.04)

Abbreviations: ICV, intraindividual coefficient of variation; N, number of subjects, RT, reaction time in ms, SD, standard deviation.
[a]Owing to the low number of errors of some subjects, their SD values could not be calculated. Therefore, N(10/10) = 26 for both drug conditions and N(9R) = 21 for methylphenidate for the ICV incorrect no-go trials. For the SPECT sample, the same subjects had to be excluded. Therefore, N(10/10) = 14 for both drug conditions and N(9R) = 18 for methylphenidate.

Pharmacogenetic Findings

Using the most stringent contrast to isolate inhibitory mechanisms in the Go/No-Go task (correct no-go > correct odd) (Chikazoe *et al*, 2009a), we found an interaction between *SLC6A3* genotype and drug condition for BOLD during successful inhibition. The interaction indicated a BOLD increase with MPH in 9R carriers, but a decrease in 10/10 homozygotes. The clusters showing this effect fall within the typical Go/No-Go network (Criaud and Boulinguez, 2013) and areas modulated by MPH during inhibition (Nandam *et al*, 2014; Pauls *et al*, 2012), including anterior cingulate and right lateralized prefrontoparieto-temporal structures. Additionally, we found interactions in the cerebellum and occipital regions.

Qualitatively similar interactions were observed in left PFC and right thalamus, when using the cognitively less specific contrast of correct no-go > go-baseline. That contrast has previously been used to study neural mechanisms of response inhibition but has recently been criticized for
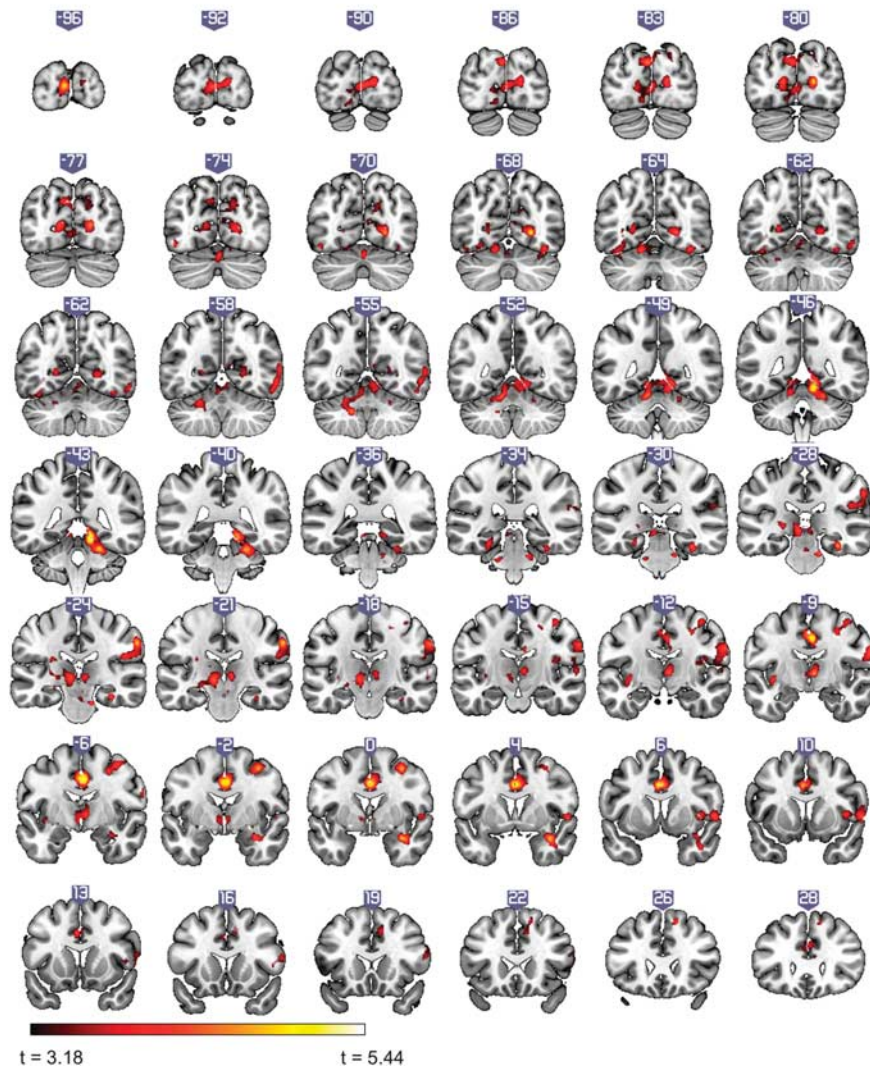
Interaction Drug x Genotype

Figure 1 Clusters showing an interaction between Genotype (9R, 10/10) and Drug (methylphenidate, placebo) in the contrast correct no-go > correct odd (family-wise error corrected (FWEc), peak voxel threshold $P < 0.001$, uncorrected). Slices in neurologic convention (right side = right side).

confounding inhibitory demands with attentional capture because of low no-go stimulus frequency (Chikazoe et al, 2009a; Criaud and Boulinguez, 2013).

Interestingly, the contrast correct no-go > incorrect no-go showed no significant pharmacogenetic effect at the chosen level of statistical significance. This finding indicates that for this specific contrast, the upregulation in putamen during incorrect no-go trials that was reported in the entire sample in Costa et al (2013b) is genotype independent.

Taken together, the current analysis and our previous data point to both genotype-dependent and genotype-independent effects of MPH. The availability of these three contrasts and their comparison concerning pharmacogenetic MPH effects paints a complex picture. It could be argued that both the correct no-go > correct odd and the correct no-go > go baseline contrasts involve the comparison of a more demanding response option (not to press the button) with a simpler, automated response option (press

the button). In contrast, the direct comparison of successful with failed no-go trials in the contrast correct no-go > incorrect no-go does not isolate this task demand factor but most likely identifies differences due to success in inhibition and the commitment and processing of an error. Therefore, it may be concluded that our pharmacogenetic effects, despite our attempt to use a cognitively specific contrast to isolate response inhibition (Chikazoe et al, 2009a), may be due in part to general factors such as task demand.

As can be seen from Figure 2, there were differences in hemodynamic response between genotype groups under placebo, indicating higher BOLD in 10/10 homozygotes than 9R carriers. These effects in the absence of pharmacologic stimulation are indicative of genotype-driven differences in baseline DA levels. However, it should be pointed out that the opposite pattern (ie, greater BOLD in 9R than 10/10) was observed in healthy participants performing a

Table 2 Areas Displaying Drug × Genotype Interactions During the Contrast Correct No-Go > Correct Odd (N = 50)

Activated region	MNI coordinates			Cluster Size	BA	Z	P_{cor}
	x	y	z				
Cerebellum R	12	−44	−14	7478	—	5.07	<0.001
Occipital Pole L	−6	−98	8		17	4.64	
Intracalcarine Cortex R	24	−68	2		18/19	4.62	
Cingulate Gyrus R	4	−8	40	1880	23	4.93	<0.001
Cingulate Gyrus R	0	4	36			4.73	
Superior Frontal Gyrus R	6	48	30		32	4.11	
Supramarginal Gyrus R	62	−22	38	1046	1	4.54	<0.001
Postcentral Gyrus R	64	−10	30		43	4.37	
Parietal Operculum R	48	−26	22		48	4.09	
Central Opercular Cortex R	56	6	2	571	44	4.11	0.001
Insular Cortex R	42	8	4		48	3.95	
Inferior Frontal Gyrus R	58	16	16		44	3.68	
Middle Frontal Gyrus R	36	−2	54	541	6	4.50	0.001
Precentral Gyrus R	38	−14	58		6	4.01	
Precentral Gyrus R	30	−6	48		6	3.99	
Occipital Fusiform Gyrus R	38	−66	−16	457	19	4.14	0.002
Middle Temporal Gyrus	58	−58	−2		37	4.09	
Middle Temporal Gyrus	62	−58	10		37	4.00	
Temporal Pole R	34	2	−22	320	36	4.52	0.012
Temporal Pole R	42	6	30		20	3.96	

Abbreviations: BA, Brodmann area; FWEc, family-wise error corrected; L, left hemisphere, P_{cor}, p-value corrected; R, right hemisphere.
Note: P_{cor} for multiple comparison on the basis of cluster extent (FWEc; peak voxel threshold $p < 0.001$ uncorrected). Anatomical regions from Harvard-Oxford Subcortical/Cortical Structural Atlas: L and R. Cluster size is given in number of voxels. Peak voxels are in italics, subclusters are indented.

stop-signal task, another measure of motor response inhibition (Congdon et al, 2009). Given the differences between stop-signal and Go/No-Go tasks (Aron, 2011), future studies are needed to clarify whether associations of SLC6A3 with brain function are reliably observed during different measures of motor response inhibition.

An interesting finding concerns the lateralization to the right hemisphere of some of our results. Specifically, both the overall activation pattern underlying correct no-go trials and the pharmacogenetic interaction effect for correct no-go compared with correct odd trials showed pronounced effects in the right, but not in the left, hemisphere. These findings may be compatible with meta-analyses indicating a predominantly right lateralized inhibition network during Go/No-Go tasks (Criaud and Boulinguez, 2013; Mostofsky and Simmonds, 2008).

Our finding of pharmacogenetic effects of MPH outside the striatum also merits discussion. Although DAT concentrations are known to be highest in the striatum (Ciliax

et al, 1999), a purely striatal mechanism cannot explain our constellation of findings including (i) the observation of SLC6A3-independent striatal effects of MPH (Costa et al, 2013b), (ii) the lack of association between MPH effects and striatal DAT as measured with SPECT in our study (see below), and (iii) the observation of SLC6A3-dependent effects outside the striatum.

Several explanations may be drawn upon to explain this pattern. First, while the DAT is most strongly expressed in the striatum, it is also reliably found in extrastriatal regions (Ciliax et al, 1999; Saba et al, 2007), with evidence of genotype dependence in the frontal cortex (Wonodi et al, 2009). This observation opens up the possibility that these extrastriatal DATs may have a role in the pharmacogenetic effects observed here, especially given previous observations of SLC6A3-related differences in the activity of cortical regions during working memory, memory recognition, and response inhibition (Bertolino et al, 2006, 2009; Congdon et al, 2009). However, there is at present no evidence of associations between SLC6A3 genotype and DAT availability in extrastriatal areas on the basis of human PET/SPECT studies. Additionally, DAT expression outside the striatum is typically quite low (Ciliax et al, 1999) and highly variable between individuals (Koch et al, 2014).

Second, an alternative explanation is that our extrastriatal pharmacogenetic effects may have arisen through downstream DA release by striatal neurons. The latter is supported by the observation that a net increase of striatal DA enhances activity in the whole cortico-striato-thalamic-cortical network (Tisch et al, 2004). A related physiologic explanation for this pattern in our data lies in the nature of the BOLD signal, which is thought to be indicative of synaptic inputs into an area, rather than its outputs (Logothetis et al, 2001). This hypothesis may thus explain why striatal DAT genotype may affect BOLD in remote areas.

Interestingly, the right thalamus was the only anatomic overlap in interaction effects between the two contrasts showing genotype-dependent MPH effects, viz successful inhibition without influences of attentional capture (correct no-go > odd) and successful inhibition with additional influences of attentional capture and stimulus frequency (correct no-go > go-baseline). This indicates that during successful inhibition, extrastriatal regions that show a rise in extracellular DA in response to MPH (Montgomery et al, 2007), such as the thalamus, are influenced by genotype irrespective of comparison condition. Cortical effects, however, appear to arise as a function of comparison contrast. This may be explained in part by the multitude of perceptual, cognitive, and motor processes that are differentially invoked in different conditions, such as stimulus appraisal, conflict monitoring, attention, error detection, response selection, and working memory (Criaud and Boulinguez, 2013), and that are controlled for to different extents using different contrasts. However, it is important to note that the general pattern of interaction, viz an increase in BOLD in 9R and a decrease in 10/10 individuals, remained the same across different regions irrespective of contrast. This suggests the possibility of contrast-dependent cortical effects driven by contrast-independent subcortical mechanisms via thalamocortical projections.
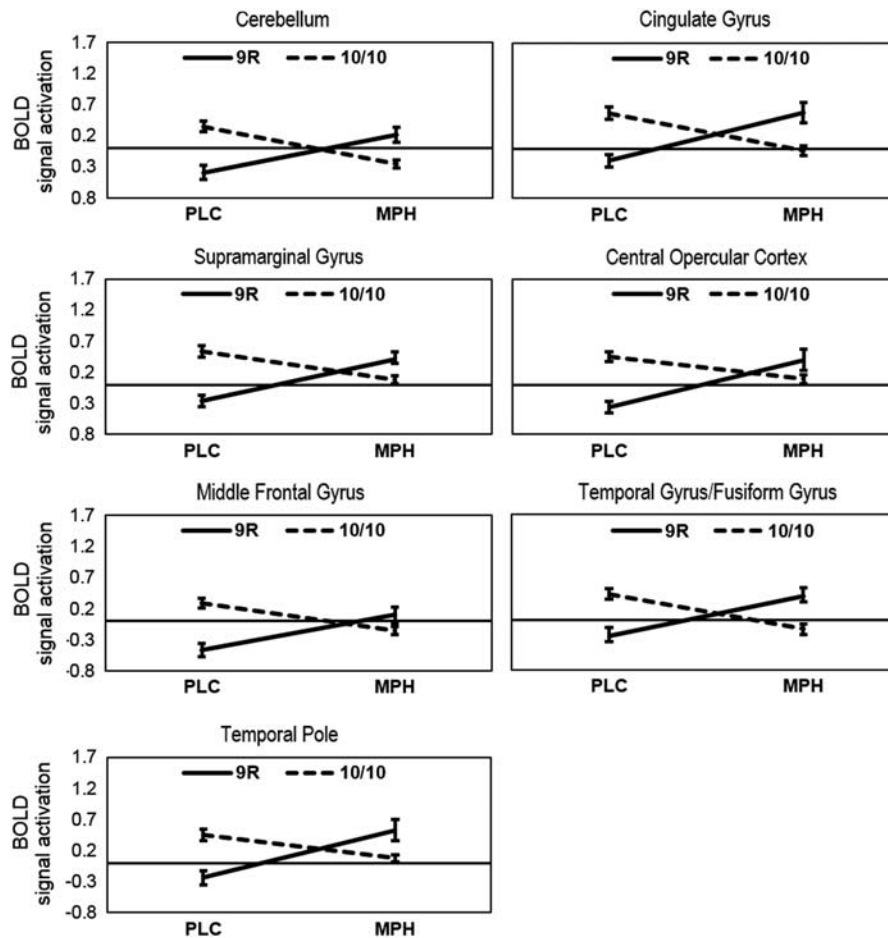
Figure 2 The interaction between Genotype (9R, 10/10) and Drug (placebo (PLC), methylphenidate (MPH)) in each of the clusters in the contrast correct no-go > correct odd (see Table 2). The y axis describes mean BOLD signal activation in the corresponding cluster. Error bars represent the SEM.

The molecular effects of the VNTR have not been fully clarified, although meta-analyses of human molecular imaging studies suggest higher DAT availability in 9R carriers (Costa *et al*, 2011; Faraone *et al*, 2014). The VNTR lies in the 3′-UTR, which is located downstream of the protein coding sequence and does not directly affect protein structure. However, the 3′-UTR may have a role in influencing posttranscriptional gene expression, for example, through transcript cleavage, mRNA stability, and localization or polyadenylation (Barrett *et al*, 2012), or remote effects from regulatory regions of other genes (Dekker, 2008).

While the precise molecular mechanisms of the effects observed here are thus still unanswered, there is converging evidence that DA-enhancing interventions lead to stronger BOLD in 9R compared with 10/10 subjects, compatible with our findings. For example, research on reward sensitivity showed that BOLD during reward anticipation and delivery, as well as during presentation of reward-related stimuli is larger for 9R carriers than 10R hetero- and homozygotes (Dreher *et al*, 2009; Forbes *et al*, 2009; Franklin *et al*, 2009). Direct support of enhanced striatal DA release in 9R carriers was obtained following smoking in a [^{11}C]raclopride PET study (Brody *et al*, 2006), in agreement with studies suggesting the 9R allele to be associated with enhanced dopaminergic output. Overall, Dreher *et al* (2009) conclude

that '9R carriers, irrespective of the investigated domain, show hyper-responsivity of specific brain networks' (p 620), compatible with our finding of greater BOLD following MPH in 9R carriers than 10/10 homozygotes (however, see Wittmann *et al*, 2013).

SPECT Findings

Irrespective of the precise molecular mechanisms, but of importance to the present study, the VNTR has in human PET and SPECT studies been related to striatal DAT availability. Meta-analyses suggest that 9R carriers have higher striatal DAT availability compared with non-9R carriers, with medium effect size (Costa *et al*, 2011; Faraone *et al*, 2014). In our sample, there was a numerical difference in the same direction with a medium effect size ($d = 0.40$).

Therefore, to provide a possible mechanism of *SLC6A3* pharmacogenetic effects, we considered striatal DAT availability obtained with ^{123}I-FP-CIT SPECT as potential predictor of MPH response. However, no significant relationships were observed. This negative finding may constitute a type II error and has to be interpreted cautiously. However, given the observation of molecular predictors of pharmacologic effects on BOLD in samples smaller than ours (Cools *et al*, 2009), we suggest on the basis of our SPECT data that

moderating effects of the VNTR on BOLD were unlikely to be because of the actual amount of striatal DAT.

Limitations

Some limitations should be noted. First, our SPECT method is limited by the semiquantitative assessment of DAT, which however is inherent to most receptor and transporter SPECT and PET studies. A further limitation is our focus on a single VNTR, which is only one of several polymorphisms thought to regulate striatal DA. Finally, the generalizability of the findings is limited to healthy, Caucasian males. This selection strategy maximizes sample homogeneity in terms of genetics and avoids influences of hormonal fluctuations in females but comes at the cost of reduced generalizability. Additionally, the negative behavioral findings might be explained by this careful screening, leading to high overall levels of performance and little variance in inhibition errors.

CONCLUSIONS

Overall, our findings suggest that catecholaminergic modulation of the neurophysiologic correlates of motor response inhibition in the Go/No-Go task is *SLC6A3* genotype-dependent. We thus build on previous studies (Clatworthy *et al*, 2009; Cools and D'Esposito, 2011) in attempting to identify predictors of the variability in response to dopaminergic drugs such as MPH, which may help improve our mechanistic understanding of this clinically relevant compound.

REFERENCES

Aron AR (2011). From reactive to proactive and selective control: developing a richer model for stopping inappropriate responses. *Biol Psychiatry* **69**: e55–e68.

Bari A, Robbins TW (2013). Inhibition and impulsivity: behavioral and neural basis of response control. *Prog Neurobiol* **108**: 44–79.

Barrett LW, Fletcher S, Wilton SD (2012). Regulation of eukaryotic gene expression by the untranslated gene regions and other non-coding elements. *Cell Mol Life Sci* **69**: 3613–3634.

Bertolino A, Blasi G, Latorre V, Rubino V, Rampino A, Sinibaldi L et al (2006). Additive effects of genetic variation in dopamine regulating genes on working memory cortical activity in human brain. *J Neurosci* **26**: 3918–3922.

Bertolino A, Fazio L, Giorgio A, Di Blasi G, Romano R, Taurisano P et al (2009). Genetically determined interaction between the dopamine transporter and the D2 receptor on prefronto-striatal activity and volume in humans. *J Neurosci* **29**: 1224–1234.

Bezdjian S, Baker LA, Lozano DI, Raine A (2009). Assessing inattention and impulsivity in children during the Go/NoGo task. *Br J Dev Psychol* **27**: 365–383.

Brody AL, Mandelkern MA, Olmstead RE, Scheibal D, Hahn E, Shiraga S et al (2006). Gene variants of brain dopamine pathways and smoking-induced dopamine release in the ventral caudate/nucleus accumbens. *Arch Gen Psychiatry* **63**: 808–816.

Chamberlain SR, Hampshire A, Müller U, Rubia K, Del Campo N, Craig K et al (2009). Atomoxetine modulates right inferior frontal activation during inhibitory control: a pharmacological functional magnetic resonance imaging study. *Biol Psychiatry* **65**: 550–555.

Chang L (1978). A method for attenuation correction in radio-nuclide computed tomography. *Nucl Sci IEEE Trans* **25**: 638–643.

Chikazoe J, Jimura K, Asari T, Yamashita K, Morimoto H, Hirose S et al (2009a). Functional dissociation in right inferior frontal cortex during performance of go/no-go task. *Cereb cortex* **19**: 146–152.

Chikazoe J, Jimura K, Hirose S, Yamashita K, Miyashita Y, Konishi S (2009b). Preparation to inhibit a response complements response inhibition during performance of a stop-signal task. *J Neurosci* **29**: 15870–15877.

Ciliax BJ, Drash GW, Staley JK, Haber S, Mobley CJ, Miller GW et al (1999). Immunocytochemical localization of the dopamine transporter in human brain. *J Comp Neurol* **409**: 38–56.

Clatworthy PL, Lewis SJG, Brichard L, Hong YT, Izquierdo D, Clark L et al (2009). Dopamine release in dissociable striatal subregions predicts the different effects of oral methylphenidate on reversal learning and spatial working memory. *J Neurosci* **29**: 4690–4696.

Coghill DR, Seth S, Pedroso S, Usala T, Currie J, Gagliano A (2014). Effects of methylphenidate on cognitive functions in children and adolescents with attention-deficit/hyperactivity disorder: evidence from a systematic review and a meta-analysis. *Biol Psychiatry* **76**: 603–615.

Cohen MX, Krohn-Grimberghe A, Elger CE, Weber B (2007). Dopamine gene predicts the brain's response to dopaminergic drug. *Eur J Neurosci* **26**: 3652–3660.

Congdon E, Constable RT, Lesch KP, Canli T (2009). Influence of SLC6A3 and COMT variation on neural activation during response inhibition. *Biol Psychol* **81**: 144–152.

Cools R, D'Esposito M (2011). Inverted-U-shaped dopamine actions on human working memory and cognitive control. *Biol Psychiatry* **69**: e113–e125.

Cools R, Frank MJ, Gibbs SE, Miyakawa A, Jagust W, D'Esposito M (2009). Striatal dopamine predicts outcome-specific reversal learning and its sensitivity to dopaminergic drug administration. *J Neurosci* **29**: 1538–1543.

Cooper JA, Sagar HJ, Tidswell P, Jordan N (1994). Slowed central processing in simple and go/no-go reaction time tasks in Parkinson's disease. *Brain* **117**: 517–529.

Costa A, Fougère C, la, Pogarell O, Möller H-J, Riedel M, Ettinger U (2013a). Impulsivity is related to striatal dopamine transporter availability in healthy males. *Psychiatry Res* **211**: 251–256.

Costa A, Riedel M, Müller U, Möller H-J, Ettinger U (2011). Relationship between SLC6A3 genotype and striatal dopamine transporter availability: a meta-analysis of human single photon emission computed tomography studies. *Synapse* **65**: 998–1005.

Costa A, Riedel M, Pogarell O, Menzel-Zelnitschek F, Schwarz M, Reiser M et al (2013b). Methylphenidate effects on neural activity during response inhibition in healthy humans. *Cereb Cortex* **23**: 1179–1189.

Criaud M, Boulinguez P (2013). Have we been asking the right questions when assessing response inhibition in go/no-go tasks with fMRI? A meta-analysis and critical review. *Neurosci Biobehav Rev* **37**: 11–23.

Dalley JW, Everitt BJ, Robbins TW (2011). Impulsivity, compulsivity, and top-down cognitive control. *Neuron* 69: 680–694.

Dekker J (2008). Gene regulation in the third dimension. *Science* 319: 1793–1794.

Dreher J-C, Kohn P, Kolachana B, Weinberger DR, Berman KF (2009). Variation in dopamine genes influences responsivity of the human reward system. *Proc Natl Acad Sci USA* 106: 617–622.

Faraone SV, Spencer TJ, Madras BK, Zhang-James Y, Biederman J (2014). Functional effects of dopamine transporter gene genotypes on *in vivo* dopamine transporter functioning: a meta-analysis. *Mol Psychiatry* 19: 880–889.

Forbes EE, Brown SM, Kimak M, Ferrell RE, Manuck SB, Hariri AR (2009). Genetic variation in components of dopamine neurotransmission impacts ventral striatal reactivity associated with impulsivity. *Mol Psychiatry* 14: 60–70.

la Fougère C, Krause J, Krause K-H, Josef Gildehaus F, Hacker M, Koch W et al (2006). Value of ^{99}mTc-TRODAT-1 SPECT to predict clinical response to methylphenidate treatment in adults with attention deficit hyperactivity disorder. *Nucl Med Commun* 27: 733–737.

la Fougère C, Pöpperl G, Levin J, Wängler B, Böning G, Uebleis C et al (2010). The value of the dopamine D2/3 receptor ligand 18F-desmethoxyfallypride for the differentiation of idiopathic and nonidiopathic parkinsonian syndromes. *J Nucl Med* 51: 581–587.

Franklin TR, Lohoff FW, Wang Z, Sciortino N, Harper D, Li Y et al (2009). DAT genotype modulates brain and behavioral responses elicited by cigarette cues. *Neuropsychopharmacology* 34: 717–728.

Gainetdinov RR, Caron MG (2003). Monoamine transporters: from genes to behavior. *Annu Rev Pharmacol Toxicol* 43: 261–284.

Gilbert DL, Wang Z, Sallee FR, Ridel KR, Merhar S, Zhang J et al (2006). Dopamine transporter genotype influences the physiological response to medication in ADHD. *Brain* 129: 2038–2046.

Goldman-Rakic PS, Muly EC, Williams GV (2000). D(1) receptors in prefrontal cells and circuits. *Brain Res Brain Res Rev* 31: 295–301.

Kambeitz J, Romanos M, Ettinger U (2014). Meta-analysis of the association between dopamine transporter genotype and response to methylphenidate treatment in ADHD. *Pharmacogenom J* 14: 77–84.

Koch W, Radau PE, Hamann C, Tatsch K (2005). Clinical testing of an optimized software solution for an automated, observer-independent evaluation of dopamine transporter SPECT studies. *J Nucl Med* 46: 1109–1118.

Koch W, Schaaff N, Pöpperl G, Mulert C, Juckel G, Reicherzer M et al (2007). [I-123] ADAM and SPECT in patients with borderline personality disorder and healthy control subjects. *J Psychiatry Neurosci* 32: 234–240.

Koch W, Unterrainer M, Xiong G, Bartenstein P, Diemling M, Varrone A et al (2014). Extrastriatal binding of [(123)I]FP-CIT in the thalamus and pons: gender and age dependencies assessed in a European multicentre database of healthy controls. *Eur J Nucl Med Mol Imag* 41: 1938–1946.

Linssen AMW, Sambeth A, Vuurman EFPM, Riedel WJ (2014). Cognitive effects of methylphenidate in healthy volunteers: a review of single dose studies. *Int J Neuropsychopharmacol* 17: 961–977.

Logothetis NK, Pauls J, Augath M, Trinath T, Oeltermann A (2001). Neurophysiological investigation of the basis of the fMRI signal. *Nature* 412: 150–157.

Loo SK, Specter E, Smolen A, Hopfer C, Teale PD, Reite ML (2003). Functional effects of the DAT1 polymorphism on EEG measures in ADHD. *J Am Acad Child Adolesc Psychiatry* 42: 986–993.

Mattay VS, Goldberg TE, Fera F, Hariri AR, Tessitore A, Egan MF et al (2003). Catechol O-methyltransferase val158-met genotype and individual variation in the brain response to amphetamine. *Proc Natl Acad Sci USA* 100: 6186–6191.

Mehta MA (2002). Where do we go from here? The importance of initial values. *Neuropsychopharmacology* 27: 879–880.

Montgomery AJ, Asselin M-C, Farde L, Grasby PM (2007). Measurement of methylphenidate-induced change in extrastriatal dopamine concentration using [^{11}C]FLB 457 PET. *J Cereb Blood Flow Metab* 27: 369–377.

Mostofsky SH, Simmonds DJ (2008). Response inhibition and response selection: two sides of the same coin. *J Cogn Neurosci* 20: 751–761.

Nandam LS, Hester R, Bellgrove MA (2014). Dissociable and common effects of methylphenidate, atomoxetine and citalopram on response inhibition neural networks. *Neuropsychologia* 56: 263–270.

Nandam LS, Hester R, Wagner J, Cummins TDR, Garner K, Dean AJ et al (2011). Methylphenidate but not atomoxetine or citalopram modulates inhibitory control and response time variability. *Biol Psychiatry* 69: 902–904.

Pauls AM, O'Daly OG, Rubia K, Riedel WJ, Williams SCR, Mehta MA (2012). Methylphenidate effects on prefrontal functioning during attentional-capture and response inhibition. *Biol Psychiatry* 72: 142–149.

Radau PE, Linke R, Slomka PJ, Tatsch K (2000). Optimization of automated quantification of ^{123}I-IBZM uptake in the striatum applied to parkinsonism. *J Nucl Med* 41: 220–227.

Rubia K, Halari R, Cubillo A, Smith AB, Mohammad A-M, Brammer M et al (2011). Methylphenidate normalizes fronto-striatal underactivation during interference inhibition in medication-naïve boys with attention-deficit hyperactivity disorder. *Neuropsychopharmacology* 36: 1575–1586.

Saba W, Valette H, Schöllhorn-Peyronneau M-A, Coulon C, Ottaviani M, Chalon S et al (2007). [^{11}C]LBT-999: a suitable radioligand for investigation of extra-striatal dopamine transporter with PET. *Synapse* 61: 17–23.

Tisch S, Silberstein P, Limousin-Dowsey P, Jahanshahi M (2004). The basal ganglia: anatomy, physiology, and pharmacology. *Psychiatr Clin N Am* 27: 757–799.

Vandenbergh DJ, Persico AM, Hawkins AL, Griffin CA, Li X, Jabs EW et al (1992). Human dopamine transporter gene (DAT1) maps to chromosome 5p15.3 and displays a VNTR. *Genomics* 14: 1104–1116.

Volkow ND, Wang GJ, Fowler JS, Logan J, Schlyer D, Hitzemann R et al (1994). Imaging endogenous dopamine competition with [^{11}C]raclopride in the human brain. *Synapse* 16: 255–262.

Weisbrod M, Kiefer M, Marzinzik F, Spitzer M (2000). Executive control is disturbed in schizophrenia: evidence from event-related potentials in a Go/NoGo task. *Biol Psychiatry* 47: 51–60.

Wittmann BC, Tan GC, Lisman JE, Dolan RJ, Düzel E (2013). Reprint of: DAT genotype modulates striatal processing and long-term memory for items associated with reward and punishment. *Neuropsychologia* 51: 2469–2477.

Wonodi I, Hong LE, Stine OC, Mitchell BD, Elliott A, Roberts RC et al (2009). Dopamine transporter polymorphism modulates oculomotor function and DAT1 mRNA expression in schizophrenia. *Am J Med Genet B* 150B: 282–289.